methods

# New fluorogenic probes for neutral and alkaline ceramidases[S]

**Mireia Casasampere,*,† Núria Bielsa,*,† Daniel Riba,* Laura Bassas,* Ruijuan Xu,§ Cungui Mao,§ Gemma Fabriàs,*,** José-Luis Abad,* Antonio Delgado,[1],*,† and Josefina Casas[1],*,****

Spanish National Research Council (CSIC),* Institute for Advanced Chemistry of Catalonia (IQAC-CSIC), Department of Biological Chemistry, Research Unit on Bioactive Molecules (RUBAM), 08034 Barcelona, Spain; Faculty of Pharmacy and Food Sciences,† Department of Pharmacology, Toxicology, and Medicinal Chemistry, Unit of Pharmaceutical Chemistry (Associated Unit to CSIC), University of Barcelona, 08028 Barcelona, Spain; Department of Medicine,§ State University of New York at Stony Brook, Stony Brook, NY 11794-8155; and Centro de Investigación Biomédica en Red (CIBEREHD),** 28029 Madrid, Spain

ORCID IDs: 0000-0001-7162-3772 (G.F.); 0000-0002-8343-9611 (J-L.A); 0000-0003-4586-6070 (A.D.); 0000-0002-7926-5209 (J.C.)

**Abstract** **New fluorogenic ceramidase substrates derived from the *N*-acyl modification of our previously reported probes (RBM14) are reported. While none of the new probes were superior to the known RBM14C12 as acid ceramidase substrates, the corresponding nervonic acid amide (RBM14C24:1) is an efficient and selective substrate for the recombinant human neutral ceramidase, both in cell lysates and in intact cells. A second generation of substrates, incorporating the natural 2-(*N*-acylamino)-1,3-diol-4-ene framework (compounds RBM15) is also reported. Among them, the corresponding fatty acyl amides with an unsaturated *N*-acyl chain can be used as substrates to determine alkaline ceramidase (ACER)1 and ACER2 activities. In particular, compound RBM15C18:1 has emerged as the best fluorogenic probe reported so far to measure ACER1 and ACER2 activities in a 96-well plate format.**—Casasampere, M., N. Bielsa, D. Riba, L. Bassas, R. Xu, C. Mao, G. Fabriàs, J-L. Abad, A. Delgado, and J. Casas. **New fluorogenic probes for neutral and alkaline ceramidases. *J. Lipid Res.* 2019.** 60: **1174–1181.**

**Supplementary key words** substrate • sphingolipids • umbelliferone • ceramides

Besides their classically accepted role as structural cell components, sphingolipids are also a well-recognized group of bioactive lipids with significant implications in cell signaling and disease (1). This is the basis of the so-called sphingolipid rheostat, in which the relative levels of sphingosine (So) and sphingosine-1-phosphate (S1P) dictate the cell fate (2). Thus, while S1P results from phosphorylation of So by specific kinases (3), the intracellular levels of So are regulated by ceramidases, a group of amidohydrolases that catalyze the hydrolysis of ceramides (Cers) into So and fatty acids (4). According to their optimum pH, ceramidases are classified as acid, neutral, or alkaline. They differ in their primary structures because they are coded by different genes. The five human ceramidases described so far, one acidic [acidic ceramidase (AC)], one neutral [neutral ceramidase (NC)], and three alkaline [alkaline ceramidases (ACERs)] differ also on their tissue distribution (5). Thus, while AC is ubiquitously expressed, NC is highly expressed in the small intestine, while the three ACERs are exclusively expressed in the skin cells. Very recently, the structure of ACER3 has been disclosed (6). Apart from their optimum pH, ceramidases show different selectivity for Cers depending on the length and degree of saturation of the *N*-acyl side chain (4). Thus, AC prefers C12 and C14 Cers and NC prefers C16 and C18 Cers, while ACER1 prefers C20 to C24 chains (7). The remaining ACERs are less selective, because ACER2 deamidates Cers with saturated acyl chains (8) as well as dihydroceramides (dhCers) with C18 and C20 monounsaturated chains (9), while ACER3 also hydrolyzes phytoceramides with unsaturated acyl chains (10).

The role of some CDases as therapeutic targets (4) raises the interest for selective CDase inhibitors and, hence, the development of efficient protocols amenable to high-throughput screening (HTS) formats. In this context, in

*This work was partially supported by Spanish Ministry of Science and Innovation Grant CTQ2017-85378-R.*

*Manuscript received 29 January 2019 and in revised form 27 March 2019.*

*Published, JLR Papers in Press, March 29, 2019*
*DOI https://doi.org/10.1194/jlr.D092759*

Abbreviations: AC, acidic ceramidase; ACER, alkaline ceramidase; Cer, ceramide; dhCer, dihydroceramide; HTS, high-throughput screening; MBCD, methyl-β-cyclodextrin; NC, neutral ceramidase; So, sphingosine; S1P, sphingosine-1-phosphate.

[1]To whom correspondence should be addressed.
e-mail: delgado@rubam.net (A.D.); fina.casas@iqac.csic.es (J.C.)

[S] The online version of this article (available at http://www.jlr.org) contains a supplement.

previous works (11, 12), a series of first generation fluorogenic substrates (RBM14) with different *N*-acyl chains (from C8 to C16) were described as efficient CDase substrates with different selectivities. However, while RBM14C12 has been characterized as an efficient AC substrate (11, 13), the remaining substrates proved less selective toward NC, another interesting therapeutic target (14) for which no selective inhibitors have been developed so far. Moreover, selective substrates for the ACERs (ACER1–3) are also lacking.

Considering the above precedents and given our continued interest in the development of selective probes for the different ceramidases, we want to report on a series of new fluorogenic substrates derived from our previously reported RBM14 probes (11–13), as well as new probes derived from a homologated version thereof (RBM15) that also incorporates the 2-(*N*-acylamino)-1,3-diol-4-ene framework present in the natural Cers (**Fig. 1**).

In order to widen the scope of our previously reported RBM14 probes (11–13), longer and/or unsaturated *N*-acyl chain amides have been used in this study, in particular those from oleic acid (C18:1-ω9), erucic acid (C22:1-ω9), and nervonic acid (C24:1-ω9). In addition, results from a recent report seem to indicate that ACER1$^{-/-}$ cells accumulate α-hydroxy eicosanoic Cer (15). Because this observation can be related with a higher selectivity of ACER1 toward this type of side chain, we have also synthesized the corresponding (*R*)- and (*S*)-*N*-(α-hydroxyeicosanoyl) amides. For the sake of comparison, the same *N*-acyl substitution patterns have been applied to the new RBM15 series (Fig. 1).

## EXPERIMENTAL PROCEDURES

### Materials

The required carboxylic acids [oleic, erucic, nervonic, and (±)-α-hydroxyeicosanoic] were obtained from commercial sources. DMEM, FBS, methyl-β-cyclodextrin (MBCD), and tetracycline were from Sigma. Zeocin was from Genaxxon Bioscience and blasticidin from CalBiochem. Opti-MEM and lipofectamine 2000 were from Invitrogen. Recombinant human NC was obtained from R&D Systems. pCMV6 plasmid harboring the mouse Acer3 (MR218055) was from OriGene and the plasmid harboring ASAH2 was kindly provided by Dr. Daniel Canals and Prof. Yussuf Hannun (Department of Medicine, State University of New York at Stony Brook, Stony Brook, NY).

### Synthesis

The probes described in this work were obtained by acylation of RBM14 (11) or RBM15 with the suitable carboxylic acid. Probe RBM15 was obtained from deprotection of the corresponding *N*-Boc precursor (RBM15-*N*-Boc), obtained as described in (16).

*Deprotection of RBM15-N-Boc.* A solution of the starting material (382 mg, 942.2 μmol) in methanol (60 ml) was treated with $CH_3COCl$ (500 μl, 27.6 mmol) and the reaction was stirred at room temperature overnight. The mixture was concentrated in vacuo and the resulting crude was flash chromatographed (silica gel) with a step gradient of DCM/methanol (from 0% to 5% methanol at 1% increments). Compound RBM15 (262 mg, 855 μmol, 91% yield) was obtained as a yellow oil; TLC (DCM:methanol, 9:1; $R_f$: 0.13); $[\alpha]_D^{25}$: −3.86 (c 1.0, methanol). IR: δ 3,322 ($\nu_{O\text{-}H}$ and $\nu_{N\text{-}H}$), 2,934 ($\nu_{CH3}$), 1,698 ($\nu_{C=O,}$ ester); $^1$H NMR ($CD_3OD$, 400 MHz): δ 7.89 (d, J = 9.5 Hz, 1H), 7.54 (d, J = 8.5 Hz, 1H), 6.97-6.89 (m, 2H), 6.25 (d, J = 9.5 Hz, 1H), 5.97 (dtd, J = 15.2, 6.8, 1.3 Hz, 1H), 5.67 (ddt, J = 15.5, 6.6, 1.5 Hz, 1H), 4.34 (ddd, J = 6.1, 4.7, 1.2 Hz, 1H), 4.16 (t, J = 6.4 Hz, 2H), 3.81 (dd, J = 11.6, 4.1 Hz, 1H), 3.68 (dd, J = 11.6, 8.2 Hz, 1H), 3.23 (dt, J = 8.6, 4.4 Hz, 1H), 2.65-2.57 (m, 2H); $^{13}$C NMR ($CDCl_3$, 400 MHz): δ 163.64, 163.31, 156.86, 145.79, 131.50, 131.31, 130.46, 114.04, 113.91, 113.22, 102.19, 70.77, 68.83, 59.48, 58.31, 32.92.

*HRMS.* Calculated for $C_{16}H_{20}NO_5^+$ $[M+H]^+$: 306.1341; Found: 306.1328.

*General method for acylation of RBM14 and RBM15.* A solution of HOBt (40 mg, 285.3 μmol), the corresponding carboxylic acid (280 μmol), and EDC (70 mg, 380.4 μmol) in anhydrous DCM (5 ml) was added dropwise to a solution of RBM14 or RBM15 (190 μmol) in DCM (5 ml) and $Et_3N$ (100 μl, equivalent to 717 μmol) under argon atmosphere. For the amides of (±)-α-hydroxyeicosanoic acids, the solution of EDC and HOBt was added dropwise over a mixture of the starting amine and the carboxylic acid. In all cases, the reaction mixture was stirred at room temperature overnight, and the mixture was concentrated in vacuo. The resultant crude was flash-chromatographed (silica gel)

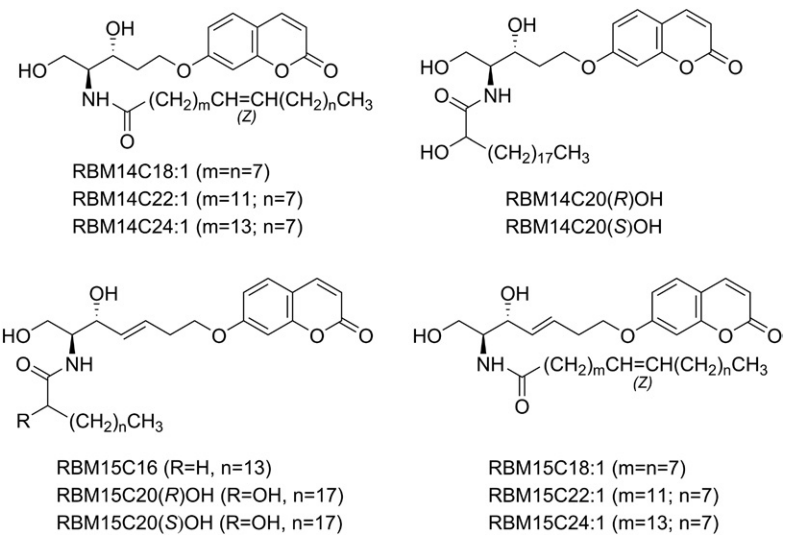


**Fig. 1.** Probes described in this work.

using a step gradient of DCM/methanol (from 0% to 3% methanol at 1% increments). The required amides were obtained as oils or waxy solids. Full characterization and NMR spectra can be found in the supplemental data.

### Cells

The FD-AC cell line stably overexpressing AC (provided by Prof. Thierry Levade, INSERM UMR1037 CRCT, Toulouse, France), HeLa T-Rex ACER1-TET-ON, HeLa T-Rex ACER2-TET-ON, HEK293T, and HT29 cells were cultured at 37°C in 5% $CO_2$ in DMEM medium supplemented with 10% FBS. The antibiotic selection of HeLa T-Rex TET-ON cells was performed with zeocin (25 μg/ml) and blasticidin (5 μg/ml). These antibiotics were removed during treatments.

### Enzyme source

Experiments with AC were performed in lysates of the FD-AC cell line stably overexpressing ASAH1. NC experiments were carried out in recombinant human NC and in HT29-overexpressing NC cells. To overexpress human NC, HT29 cells were transfected with 2.5 μg/well of a plasmid harboring the ASAH2 gene using 5 μl/well lipofectamine and Opti-MEM, following the manufacturer's instructions. Then, tetracycline (0.05 μM) was added for 24 h before use. In the case of ACERs, microsomes from three different cell lines were used. To overexpress mouse ACER3, HEK293T cells were transfected with 2.5 μg/well of a plasmid harboring the mouse ACER3 gene using 5 μl/well lipofectamine and Opti-MEM, following the manufacturer's instructions. To overexpress ACER1 and ACER2, tetracycline (0.05 μM) was added to HeLa T-Rex TET-ON cells for 24 h before use.

### Cell lysates

Cell pellets were resuspended in the appropriate volume of a 0.25 M saccharose solution with the protease inhibitors, aprotinin (1 mg/ml), leupeptin (1 mg/mml), and PMSF (100 mM). The suspension was submitted to three cycles of a 5 s sonication (probe) at 10 watts/5 s resting on ice. The cell lysate was centrifuged at 600 *g* for 5 min. The supernatant was collected, and protein concentration was determined as specified below.

### Microsomal preparations

Cell lysates obtained from HeLa T-Rex ACER1-TET-ON, HeLa T-Rex ACER2-TET-ON, and HEK293T-overexpressing ACER3 cells were transferred to ultracentrifuge tubes and spun at 100,000 *g* for 1 h at 4°C. Pellets were resuspended in a 0.25 M saccharose solution and protein concentration was determined as specified below.

### Determination of protein concentration

Protein concentrations were determined with BSA as a standard using a BCA protein determination kit (Thermo Scientific) according to the manufacturer's instructions.

### Ceramidase activities

Activity assays were carried out in 96-well plates at a final volume of 100 μl/well. Reaction buffers were: 25 mM sodium acetate buffer pH 4.5 (AC); 50 mM HEPES, 150 mM NaCl, and 1% sodium cholate (NaChol) pH 7.4 (NC); and 50 mM HEPES and 1 mM $CaCl_2$ pH 9 (ACERs). The reaction mixtures contained 25 μl/well of protein (recombinant NC or cell lysate) and 75 μl/well of substrate. Substrates were tested at 40 μM concentration, prepared from 4 mM stock solutions in ethanol. The reaction mixture was incubated at 37°C for 3 h, except for the determination of $K_M$ and $V_{max}$ parameters (between 20 and 60 min, depending on the substrate). For the determination of ceramidase activity with RBM14 substrates, reactions were stopped with 25 μl/well of methanol and then 100 μl/well of $NaIO_4$ (2.5 mg/ml in glycine-NaOH buffer, pH 10.6) were added. After incubation at 37°C for 30 min in the dark, 100 μl/well of 0.1 M glycine-NaOH buffer (pH 10.6) were added. To determine ceramidase activity with RBM15 substrates, reactions were stopped with 50 μl/well of $NaIO_4$ (2.5 mg/ml in methanol) and then 100 μl/well of KOH-methanol were added (0.1 M KOH-methanol solution in the case of NC and ACERs or 0.2 M KOH-methanol for AC). After incubation at 37°C for 30 min in the dark, 50 μl/well of 0.1 M glycine-NaOH buffer (pH 10.6) were added. In all cases, fluorescence was measured spectrophotometrically at excitation and emission wavelengths of 355 and 460 nm, respectively. The same reaction mixtures without enzymes were used as blanks.

### Ceramidase activity in intact cells

To determine ceramidase activity in intact cells, $5 \times 10^5$ cells per well were seeded in a 12-well plate. HT29 cells were transfected with 1 μg/well of a plasmid harboring the ASAH2 gene using 2 μl/well lipofectamine and Opti-MEM, following the manufacturer's instructions. Then tetracycline (0.05 μM) was added for 24 h before use. Medium was replaced by MBCD at 1, 5, and 10 mM in DMEM with NaChol (500 μM) for 30 min. Then RBM14-C24:1 was added at a final concentration of 40 μM. The plate was incubated for 3 h at 37°C in 5% $CO_2$. The reaction was stopped with 125 μl/well of methanol and then 500 μl/well of $NaIO_4$ (2.5 mg/ml in glycine-NaOH buffer, pH 10.6) were added. After incubation at 37°C for 1 h in the dark, 500 μl/well of 0.1 M glycine-NaOH buffer (pH 10.6) were added and fluorescence was measured spectrophotometrically at excitation and emission wavelengths of 355 and 460 nm, respectively. The same reaction mixtures without cells were used as blanks.

### Statistics

Comparison between two means has been carried out with the unpaired two-tailed *t*-test and statistical differences are marked with asterisks. For comparison of more than two means, data have been analyzed by one-way ANOVA followed by Bonferroni's multiple comparison test. Statistical differences between means are pointed out with different letters atop each bar (same letter indicates no statistical difference).

## RESULTS

### Design and synthesis of the probes

Probes RBM14 were obtained by *N*-acylation of the free base with the required carboxylic acids, following previously reported protocols (12, 13). Probes RBM15 were inspired in our "second generation" probes for S1P lyase, in which the installation of a vinyl unit between the amino diol moiety and the umbelliferone reporter led to a significant increase of affinity, probably due to the closer similarity of the vinylogated probe with the natural substrate (16). The retro oxa-Michael reaction required for the release of the fluorescent reporter from probes RBM15 can be promoted under basic conditions (see below) by abstraction of one of the γ-protons of the intermediate aldehyde RBM7-083 (16) resulting from $NaIO_4$ oxidation of the amino diol RBM15 arising from hydrolysis of the probe by the target ceramidase (**Fig. 2**).

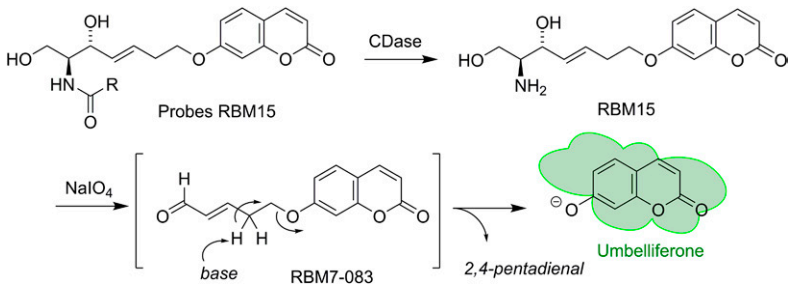


**Fig. 2.** Metabolic degradation of probes RBM15 and release of umbelliferone after oxidation of the free base and treatment of the transient aldehyde RBM7-083 with a base.

### Optimization conditions for umbelliferone release

Unlike our previously reported protocol with substrates RBM14 (11–13), the standard Gly-NaOH buffer (pH 10.6) proved inefficient to promote the complete release of the umbelliferone from the transient aldehyde RBM7-083 arising from oxidation of the aminodiol RBM15 (Fig. 2). Harsher basic conditions were required in this case to ensure acceptable levels of umbelliferone. The optimized conditions from RBM15 required the use of 0.2 M KOH-methanol (for AC) or 0.1 M KOH-methanol (for NC and ACERs), followed by a 30 min incubation at 37°C in the dark, prior to the addition of 0.2 M glycine-NaOH buffer (pH 10.6) (50 μl/well). However, even under these optimized conditions, a fluorescence of around 65% of the theoretical maximum was observed (supplemental Fig. S2).

### Probes RBM14 and RBM15 as AC substrates

Probes RBM14 and RBM15 (Fig. 1) were tested as AC substrates in FD-AC cell lysates overexpressing AC. These probes were compared with RBM14C12, reported as AC substrate in previous work (12, 13). None of the new RBM14 probes were superior to RBM14C12 as AC substrates in lysates from FD-AC cells, as evidenced by the fluorescence values observed for the released umbelliferone (**Fig. 3A**). This was also true for probes RBM15, because RBM15C16, the best AC substrate of this series, gave values around three times lower than those from RBM14C12 (Fig. 3B). These results are in agreement with the known preference of AC for C12–C14 Cers (7) and also with the fact that long-chain Cers are not AC substrates (17).

### Probes RBM14 and RBM15 as NC substrates

Probes RBM14 and RBM15 were tested as substrates in human recombinant NC and HT29 cell lysates overexpressing NC and compared with RBM14C16, which was reported in a previous article as the most efficient NC substrate among the RBM14 probes (12). In all the experiments, similar results were obtained with recombinant NC (Fig. 3C, D) and with cell lysates (Fig. 3E, F), although the corresponding C16 and C18:1 probes of both series (RBM14 and RBM15) were somewhat better substrates in cell lysates, in comparative terms with the remaining probes. The kinetic parameters in human recombinant NC are shown in **Table 1**. Among RBM14 substrates, RBM14C24:1 proved slightly superior in terms of affinity ($K_M$) and efficiency ($K_{cat}$). The preference of human recombinant NC for this *N*-acyl side chain was surprising, given the preference of the enzyme for C16 and C18 Cers (7, 18). On the other hand, the vinylogated probes RBM15 showed a slightly lower affinity in comparison with the corresponding RBM14 probes, albeit with similar or even superior $K_{cat}/K_M$ parameters. Interestingly, despite the vinylogated probes RBM15 being generally well tolerated by human recombinant NC, a striking drop in affinity was observed for RBM15C16, with $K_M$ >250. Finally, both (*R*)- and (*S*)-α-hydroxyeicosanoyl amides were well tolerated by NC, which showed a slight selectivity, in terms of $K_{cat}$, for the (*R*) isomer in the RBM15 series.

### Probes RBM14 and RBM15 as ACER substrates

Three different ACERs have been reported with an optimum activity at around pH 9. Because NC exhibits some residual CDase activity at basic pH, ACER-overexpressing systems were used to test the ability of our probes to act as ACER substrates. In a previous work (12), we showed that RBM14 probes of short to medium *N*-acyl chain lengths (C8 to C16) were inactive as ACER1 and ACER2 substrates, showing only a moderate activity as ACER3 substrates. In this work, RBM14 analogs with longer saturated or unsaturated *N*-acyl chains were devoid of activity as substrates toward all three ACER-overexpressing systems (**Fig. 4**; supplemental Fig. S3A, C, E). However, the vinylogated probes RBM15 have been revealed as new ACER1 and ACER2 substrates, being practically inactive toward ACER3. Only RBM15C16 behaved as an ACER3 substrate, although weaker than its RBM14 counterpart (Fig. 3; supplemental Fig. S3B, D, F). Overall, probes RBM15 having a long unsaturated *N*-acyl chain (18:1 and 22:1) can be used as substrates to determine ACER1 and ACER2 activities.

### Selectivity of probe RBM14C24:1 for NC

The probe RBM14C24:1 turned out to be one of the best substrates in kinetic terms on the recombinant human NC (**Fig. 5**) with the lowest $K_M$ and a high $K_{cat}/K_M$ ratio, compared with the rest of substrates tested (Table 1), and a high selectivity for NC (Fig. 5A). The above promising results prompted us to test this substrate in intact HT29 cells. However, no activity was observed after the initial assays (results not shown), which was attributed to the inability of the probe to cross the cell membrane. Encapsulation into liposomes, similarly as reported by us for a related probe (16), was not feasible due to the low solubility of RBM14C24:1 in the required solvent system. Gratifyingly, the use of MBCD, a well-known system used to increase the solubility of nonpolar substances, such as fatty acids, lipids,

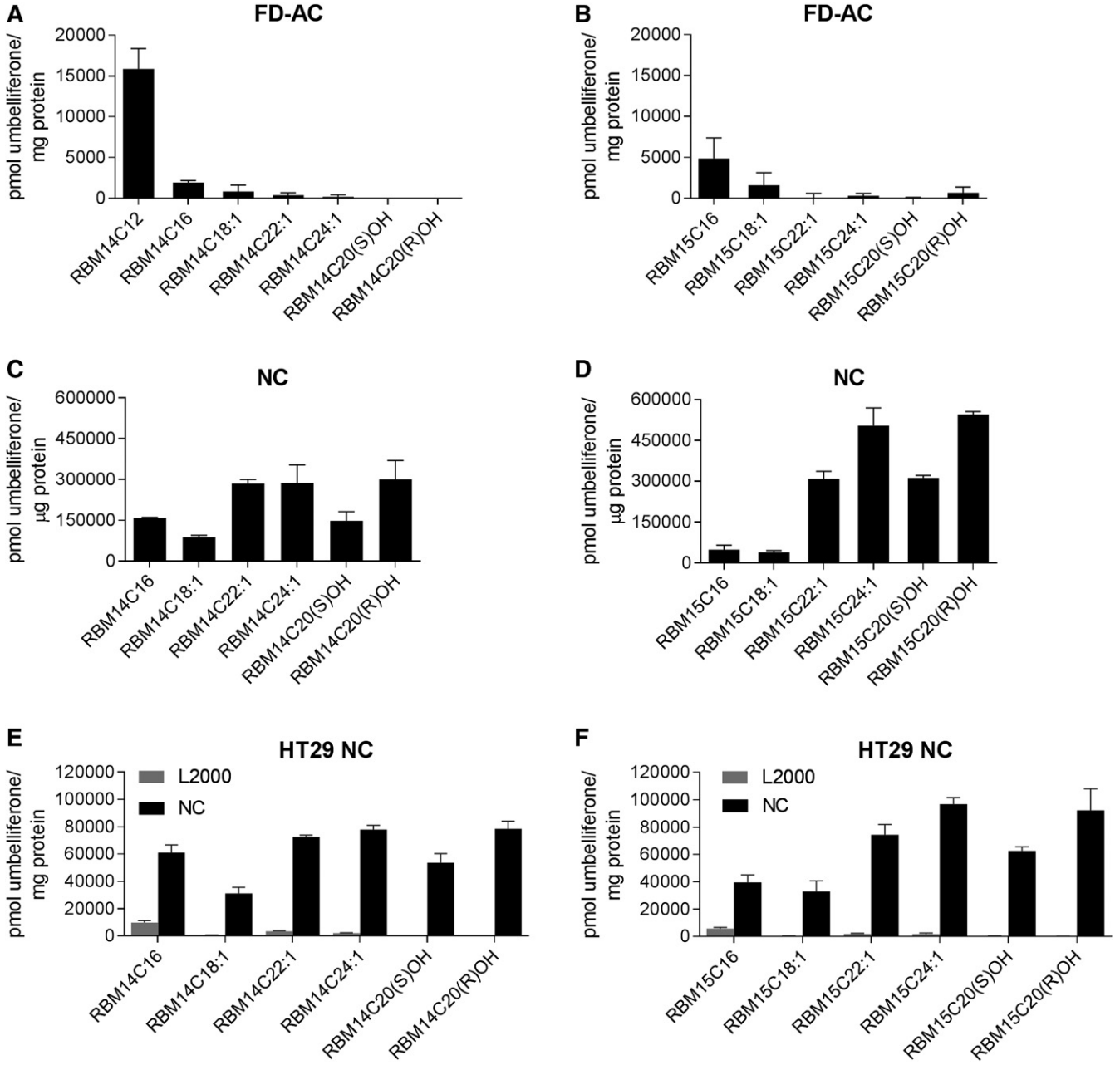


**Fig. 3.** Determination of AC (A, B) and NC (C–F) activity using RBM14 and RBM15 substrates. AC activity was measured in cell lysates from FD-AC-overexpressing cells. Incubations were carried out with RBM14 (A) or RBM15 (B) substrates in 25 mM sodium acetate buffer pH 4.5. NC activity was measured in recombinant NC (C, D) or cell lysates from HT29 control cells (L2000) and HT29 overexpressing ASAH2 (NC) (E, F). Incubations were carried out with RBM14 (C, E) or RBM15 (D, F) substrates in 50 mM HEPES, 150 mM NaCl, and 1% sodium cholate pH 7.4. New RBM14 substrates were compared with RBM14C12 (for AC) and RBM14C16 (for NC). Data correspond to the mean ± SD of at least three different experiments with triplicates.

vitamins, and cholesterol, in several cell culture applications (19) proved efficient to allow the use of RBM14C24:1 as NC substrate in intact cells (Fig. 5B). A concentration-dependent effect for MBCD was observed, and an optimal concentration of 5 mM could be established.

## DISCUSSION

Cer is considered the hub of the intricate set of pathways that are implicated in the biosynthesis and degradation of sphingolipids (20). Apart from the biosynthesis from simple structural moieties in the so-called de novo pathway, Cer can also be generated by the degradation of complex sphingolipids. Moreover, Cer, as well as dhCer (21), can also be degraded by CDases, a type of amido hydrolases that selectively convert Cers and dhCers into So and sphinganine, respectively, by hydrolysis of the *N*-fatty acyl chain present in the above sphingolipids. Interestingly, the removal of the *N*-acyl chain is important not only to control the relative levels of sphingolipids inside the cell but also to dramatically alter their intracellular mobility as a result of

TABLE 1. Kinetic parameters for the NC catalyzed hydrolysis of substrates RBM14 and RBM15

| Probe | $K_M$ | $K_{cat}$ | $K_{cat}/K_M$ |
|---|---|---|---|
| RBM14C16 | 16 ± 3.3[a] | 3,281 ± 298 | 205.1 |
| RBM14C18:1 | 28 ± 3.0 | 432 ± 64 | 15.4 |
| RBM14C20(S)OH | 14 ± 0.2 | 3,075 ± 61 | 219.6 |
| RBM14C20(R)OH | 16 ± 1.7 | 2,655 ± 317 | 165.9 |
| RBM14C22:1 | 28 ± 6.5 | 1,397 ± 219 | 49.9 |
| RBM14C24:1 | 8 ± 1.7 | 1,581 ± 100 | 197.6 |
| RBM15C16 | > 250 | — | — |
| RBM15C18:1 | 139 ± 7.2 | 3,761 ± 465 | 27.1 |
| RBM15C20(S)OH | 21 ± 1.9 | 7,257 ± 1,092 | 345.6 |
| RBM15C20(R)OH | 42 ± 0.02 | 22,954 ± 1,004 | 546.5 |
| RBM15C22:1 | 33 ± 1.7 | 4,977 ± 515 | 150.8 |
| RBM15C24:1 | 40 ± 0.9 | 8,415 ± 1,282 | 210.4 |

$K_M$ is given in micromol, $K_{cat}$ as $10^{-3}$ $s^{-1}$, and $K_{cat}/K_M$ as $M^{-1}$ $s^{-1}$. Recombinant NC (5 ng) was incubated between 20 and 60 min (depending on the substrate) at graded concentrations. Experiments were carried out as described in the methodology. Data are mean ± SD of three to five independent experiments with triplicates.

[a]See (12).

the changes in the physical properties after *N*-deacylation (22). Among the different CDases, overexpression of NC has been implicated in colon carcinogenesis (14) and, hence, has emerged as a new therapeutic target. In this context, the discovery of selective inhibitors of this enzyme should be boosted by the development of efficient sensitive analytical methods amenable for HTS protocols. Based on our previous works addressed at the development of fluorogenic probes for CDases (11–13), we were interested in expanding the scope and selectivity of our first generation probes (RBM14) by using alternative *N*-acyl chains, based on the reported preferences of CDases for the different *N*-acyl Cers. Based on these premises, a collection of potential RBM14 substrates has been synthesized and tested on our different CDase models. Interestingly, despite NC being selective for C16 and C18 Cers (10), the *N*-acyl unsaturated probe RBM14C24:1 emerged as the first selective NC substrate for recombinant human NC (Table 1, Fig. 5A). Moreover, by using MBCD as adjuvant, this substrate is also suitable to measure NC activity in intact cells. The fact that the C24:1 acyl chain of nervonic acid increases the selectivity of RBM14 probes toward NC is in full agreement with the reported structural data for this enzyme in which a 20 Å deep hydrophobic active site pocket determines the higher selectivity of NC toward long-chain acyl Cer substrates (23).

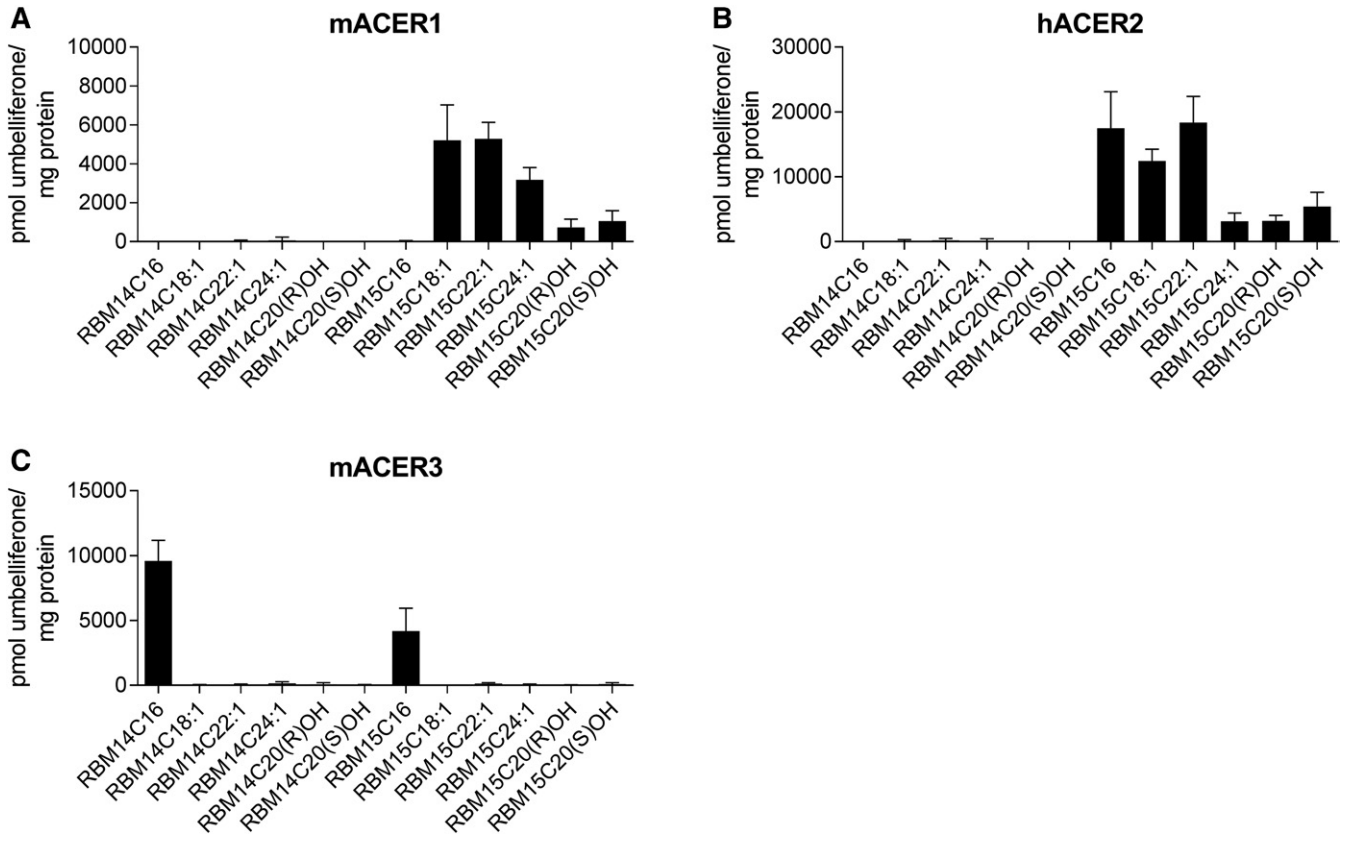


**Fig. 4.** Determination of ACER1 (A), ACER2 (B), and ACER3 (C) activity using RBM14 and RBM15 substrates. A: ACER1 activity was measured in microsomes isolated from mouse HeLa T-Rex ACER1-TET-ON cells grown in the absence or presence of tetracycline (10 ng/ml) for 24 h. Incubations were carried out with RBM14 or RBM15 substrates in 50 mM HEPES buffer with 1 mM $CaCl_2$ at pH 9. B: ACER2 activity was measured in microsomes isolated from human HeLa T-Rex ACER2-TET-ON cells grown in the absence or presence of tetracycline (10 ng/ml) for 24 h. Incubations were carried out with RBM14 or RBM15 substrates in 50 mM HEPES buffer with 1 mM $CaCl_2$ at pH 9. C: ACER3 activity was measured in microsomes isolated from mouse HEK293T control cells or HEK293T ACER3-overexpressing cells. Incubations were carried out with RBM14 or RBM15 substrates in 50 mM HEPES buffer with 1 mM $CaCl_2$ at pH 9. Hydrolysis of RBM14C16 (12) by the different ACERs is also shown for comparison. Data correspond to the mean ± SD of at least three different experiments with triplicates. Data correspond to difference between control cells and ACER-overexpressing cells (see also supplemental Fig. S3).

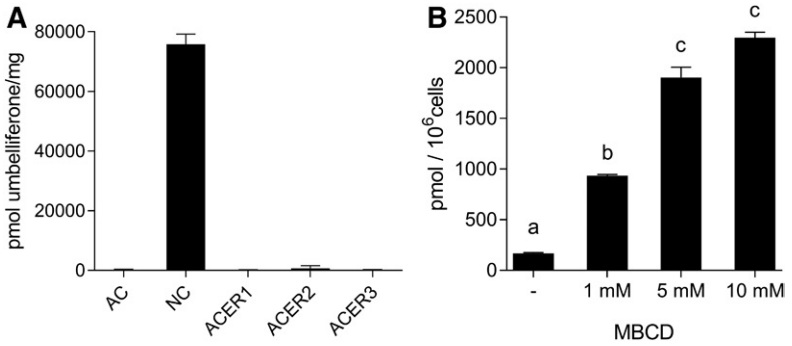


**Fig. 5.** Hydrolysis of RBM14C24:1 by CDase. A: Incubations with RBM14C24:1 were carried out with cell lysates (AC and NC) or microsomes (ACERs) at acid, neutral, or alkaline pH, as described in the Experimental Procedures. The amount (picomoles) of umbelliferone released from RBM14C24:1 was measured. Data (mean ± SD) were obtained from three different experiments with triplicates. B: NC activity in intact cells using RBM14C24:1 as substrate. HT29 cells were incubated for 30 min with MBCD at different concentrations in DMEM with NaChol (500 μM), followed by 3 h treatment with 40 μM of RBM14C24:1. Non-MBCD-treated cells were also tested. The amount (picomoles) of umbelliferone released from RBM14C24:1 was measured. Data correspond to the mean ± SD of two different experiments with duplicates. Data were analyzed by one-way ANOVA ($P < 0.0001$) followed by Bonferroni's multiple comparison test. Different letters denote a statistically significant difference between groups ($P < 0.05$).

Based on these considerations, the C24:1 acyl chain would be too long to fit into the 13 Å cavity found in the AC active site (24).

To further expand the applicability of our probes, we designed a second generation set of potential substrates (compounds RBM15, see Fig. 1). As a differential feature, these modified substrates incorporate the characteristic C4-C5 vinyl unit present in the natural Cers. Because probes RBM15 can be regarded as the vinylogated analogs of probes RBM14, their design also fits into the essence of the well-established principle of vinylogy (25). In our effort to find selective CDase substrates, probes RBM15 were tested in our five CDase models and compared with the corresponding RBM14 counterparts. The most interesting results were obtained with probes RBM15 having long unsaturated *N*-acyl chains (18:1 and 22:1), which behaved as useful ACER1 and ACER2 substrates (Fig. 4A, B) and were totally devoid of activity on AC (Fig. 3A, B) and ACER3 (Fig. 4C). Because RBM15C18:1 showed much weaker activity as NC substrate (Fig. 3C-F), this probe has emerged as the best fluorogenic probe reported so far to measure ACER1 and ACER2 activities in a 96-well plate format. Although less studied than other CDases, recent studies have shown the implication of ACER1 in mammalian skin homeostasis and whole-body energy homeostasis (26) and that of ACER2 in DNA damage (27) and cell differentiation processes (28).

In summary, the fluorogenic probes reported in this work complement our previously reported probe for AC (RBM14C12) (11–13) by enlarging the scope of applicability with the discovery of RBM14C24:1 as a highly selective probe for NC and probe RBM15C18:1 for ACER1 and ACER2 with very low NC activity. These results represent a valuable addition to the available toolkit of fluorogenic CDase substrates and may enable the development of efficient HTS protocols for the screening of potential selective inhibitors of this relevant group of amidohydrolases.

The authors acknowledge the experimental contributions from Mr. Alex García and Mr. Pedro Rayo.

## REFERENCES

1. Hannun, Y. A., and L. M. Obeid. 2018. Sphingolipids and their metabolism in physiology and disease. *Nat. Rev. Mol. Cell Biol.* **19:** 175–191.
2. Newton, J., S. Lima, M. Maceyka, and S. Spiegel. 2015. Revisiting the sphingolipid rheostat: evolving concepts in cancer therapy. *Exp. Cell Res.* **333:** 195–200.
3. Sanllehí, P., J. L. Abad, J. Casas, and A. Delgado. 2016. Inhibitors of sphingosine-1-phosphate metabolism (sphingosine kinases and sphingosine-1-phosphate lyase). *Chem. Phys. Lipids.* **197:** 69–81.
4. Coant, N., W. Sakamoto, C. Mao, and Y. A. Hannun. 2017. Ceramidases, roles in sphingolipid metabolism and in health and disease. *Adv. Biol. Regul.* **63:** 122–131.
5. Mao, C., and L. M. Obeid. 2008. Ceramidases: regulators of cellular responses mediated by ceramide, sphingosine, and sphingosine-1-phosphate. *Biochim. Biophys. Acta.* **1781:** 424–434.
6. Vasiliauskaité-Brooks, I., R. D. Healey, P. Rochaix, J. Saint-Paul, R. Sounier, C. Grison, T. Waltrich-Augusto, M. Fortier, F. Hoh, E. M. Saied, et al. 2018. Structure of a human intramembrane ceramidase explains enzymatic dysfunction found in leukodystrophy. *Nat. Commun.* **9:** 5437.
7. Mao, C., R. Xu, Z. M. Szulc, A. Bielawska, S. H. Galadari, and L. M. Obeid. 2001. Cloning and characterization of a novel human alkaline ceramidase: a mammalian enzyme that hydrolyzes phytoceramide. *J. Biol. Chem.* **276:** 26577–26588.
8. Sun, W., J. Jin, R. Xu, W. Hu, Z. M. Szulc, J. Bielawski, L. M. Obeid, and C. Mao. 2010. Substrate specificity, membrane topology, and activity regulation of human alkaline ceramidase 2 (ACER2). *J. Biol. Chem.* **285:** 8995–9007.
9. Mao, Z., W. Sun, R. Xu, S. Novgorodov, Z. M. Szulc, J. Bielawski, L. M. Obeid, and C. Mao. 2010. Alkaline ceramidase 2 (ACER2) and its product dihydrosphingosine mediate the cytotoxicity of N-(4-hydroxyphenyl)retinamide in tumor cells. *J. Biol. Chem.* **285:** 29078–29090.
10. Hu, W., R. Xu, W. Sun, Z. M. Szulc, J. Bielawski, L. M. Obeid, and C. Mao. 2010. Alkaline ceramidase 3 (ACER3) hydrolyzes unsaturated long-chain ceramides, and its down-regulation inhibits both cell proliferation and apoptosis. *J. Biol. Chem.* **285:** 7964–7976.
11. Bedia, C., J. Casas, V. Garcia, T. Levade, and G. Fabrias. 2007. Synthesis of a novel ceramide analogue and its use in a high-throughput fluorogenic assay for ceramidases. *ChemBioChem.* **8:** 642–648.

12. Casasampere, M., L. Camacho, F. Cingolani, J. Casas, M. Egido-Gabás, J. L. Abad, C. Bedia, R. Xu, K. Wang, D. Canals, et al. 2015. Activity of neutral and alkaline ceramidases on fluorogenic N-acylated coumarin-containing aminodiols. *J. Lipid Res.* **56:** 2019–2028.
13. Bedia, C., L. Camacho, J. L. Abad, G. Fabrias, and T. Levade. 2010. A simple fluorogenic method for determination of acid ceramidase activity and diagnosis of Farber disease. *J. Lipid Res.* **51:** 3542–3547.
14. García-Barros, M., N. Coant, T. Kawamori, M. Wada, A. J. Snider, J. P. Truman, B. X. Wu, H. Furuya, C. J. Clarke, A. B. Bialkowska, et al. 2016. Role of neutral ceramidase in colon cancer. *FASEB J.* **30:** 4159–4171.
15. Lin, C-L., R. Xu, J. K. Yi, F. Li, J. Chen, E. C. Jones, J. B. Slutsky, L. Huang, B. Rigas, J. Cao, et al. 2017. Alkaline ceramidase 1 protects mice from premature hair loss by maintaining the homeostasis of hair follicle stem cells. *Stem Cell Reports.* **9:** 1488–1500.
16. Sanllehí, P., M. Casasampere, J-L. Abad, G. Fabriàs, O. López, J. Bujons, J. Casas, and A. Delgado. 2017. The first fluorogenic sensor for sphingosine-1-phosphate lyase activity in intact cells. *Chem. Commun. (Camb.).* **53:** 5441–5444.
17. Momoi, T., Y. Ben-Yoseph, and H. L. Nadler. 1982. Substrate-specificities of acid and alkaline ceramidases in fibroblasts from patients with Farber disease and controls. *Biochem. J.* **205:** 419–425.
18. El Bawab, S., A. Bielawska, and Y. A. Hannun. 1999. Purification and characterization of a membrane-bound nonlysosomal ceramidase from rat brain. *J. Biol. Chem.* **274:** 27948–27955.
19. Uekama, K. 2004. Design and evaluation of cyclodextrin-based drug formulation. *Chem. Pharm. Bull. (Tokyo).* **52:** 900–915.
20. Hannun, Y. A., and L. M. Obeid. 2011. Many ceramides. *J. Biol. Chem.* **286:** 27855–27862.
21. Fabrias, G., J. Munoz-Olaya, F. Cingolani, P. Signorelli, J. Casas, V. Gagliostro, and R. Ghidoni. 2012. Dihydroceramide desaturase and dihydrosphingolipids: debutant players in the sphingolipid arena. *Prog. Lipid Res.* **51:** 82–94.
22. Hannun, Y. A., and L. M. Obeid. 2008. Principles of bioactive lipid signalling: lessons from sphingolipids. *Nat. Rev. Mol. Cell Biol.* **9:** 139–150.
23. Airola, M. V., W. J. Allen, M. J. Pulkoski-Gross, L. M. Obeid, R. C. Rizzo, and Y. A. Hannun. 2015. Structural basis for ceramide recognition and hydrolysis by human neutral ceramidase. *Structure.* **23:** 1482–1491.
24. Gebai, A., A. Gorelik, Z. Li, K. Illes, and B. Nagar. 2018. Structural basis for the activation of acid ceramidase. *Nat. Commun.* **9:** 1621.
25. Krishnamurthy, S. 1982. The principle of vinylogy. *J. Chem. Educ.* **59:** 543–547.
26. Liakath-Ali, K., V. E. Vancollie, C. J. Lelliott, A. O. Speak, D. Lafont, H. J. Protheroe, C. Ingvorsen, A. Galli, A. Green, D. Gleeson, et al. 2016. Alkaline ceramidase 1 is essential for mammalian skin homeostasis and regulating whole-body energy expenditure. *J. Pathol.* **239:** 374–383.
27. Xu, R., K. Wang, I. Mileva, Y. A. Hannun, L. M. Obeid, and C. Mao. 2016. Alkaline ceramidase 2 and its bioactive product sphingosine are novel regulators of the DNA damage response. *Oncotarget.* **7:** 18440–18457.
28. Sun, W., R. Xu, W. Hu, J. Jin, H. A. Crellin, J. Bielawski, Z. M. Szulc, B. H. Thiers, L. M. Obeid, and C. Mao. 2008. Upregulation of the Human Alkaline Ceramidase 1 and Acid Ceramidase Mediates Calcium-Induced Differentiation of Epidermal Keratinocytes. *J. Invest. Dermatol.* **128:** 389–397.